

Devil's Staircase and Disorder Transitions in Sliding Vortices and Wigner Crystals on Random Substrates with Transverse Driving

C. Reichhardt and C.J. Olson Reichhardt

Theoretical Division, Los Alamos National Laboratory, Los Alamos, New Mexico 87545

(Dated: March 23, 2022)

Using numerical simulations we show that, in the presence of random quenched disorder, sliding superconducting vortices and Wigner crystals pass through a variety of dynamical phases when an additional transverse driving force is applied. If the disorder is weak, the driven particles form a moving lattice and the transverse response shows a devil's staircase structure as the net driving force vector locks with the symmetry directions of the moving lattice, in agreement with the predictions of Le Doussal and Giamarchi. For strong disorder, and particularly for smoothly varying potential landscapes, the transverse response consists of a sequence of disordering transitions with an intervening formation of stable channel structures.

PACS numbers: 74.25.Qt

I. INTRODUCTION

A number of systems, including moving vortex lattices in type-II superconductors with disordered pinning [1, 2, 3], sliding charge-density waves [4], and driven Wigner crystals [5], can be modeled as moving lattices interacting with random quenched disorder. If the external driving force is weak the particles are pinned, while at high external drives the particles can slide. There is extensive evidence that in the sliding phase the particles organize into a moving anisotropic crystal or moving smectic phase and that the motion is confined to well defined channels [1, 2, 3, 6, 7, 8, 9]. A remarkable property of these channels is that if an additional external drive is applied in the *transverse* direction the moving system exhibits a finite transverse depinning threshold [2]. This transverse depinning threshold has been confirmed in a number of simulations [5, 6, 7, 8, 10] and experiments [9].

A transverse depinning barrier is also present for particles moving over a periodic substrate. In this type of system, the transverse velocity force curves exhibit a devil's staircase structure as the particle motion locks to the symmetry directions of the periodic substrate [11, 12, 13]. This effect occurs even for a single particle moving over a periodic substrate [14, 15, 16]. In contrast, a single particle moving over a random substrate will not show a transverse depinning threshold or a devil's staircase response.

In Ref. [2], a finite transverse depinning force was predicted for a vortex lattice, and it was also conjectured that a moving lattice would align with the direction of the initial longitudinal drive in order to minimize power dissipation. If the moving lattice remains aligned in this initial orientation as a transverse drive is applied, the transverse velocity force curves could exhibit a devil's staircase response as the applied force vector locks with the triangular symmetry of the moving lattice. In contrast to a system with a periodic substrate, here the symmetry breaking which leads to the preferred directions of motion comes from the moving lattice itself. Numerically

observing the devil's staircase in a system with random disorder can be difficult since large systems and long time averages of the transverse velocity are needed to reduce the fluctuations. An added difficulty with observing this type of devil's staircase is that fine increments of the applied transverse force are required to resolve the higher order steps.

Another possibility for the dynamics at the transverse depinning transition which has not been considered is that the moving lattice structure could become strongly disordered at the depinning transition, leading to plastic distortions. If such a *plastic transverse depinning* occurs, it is natural to ask if the particles would reorder into a tilted channel structure, causing a new transverse barrier to develop.

II. SIMULATION

A. Vortex System

To address these issues we consider two types of two-dimensional (2D) systems with periodic boundary conditions. The first is a vortex system containing N_v vortices and N_p short range random pinning sites. The vortices are modeled as point particles and their dynamics evolve via an overdamped equation of motion, given for vortex i as

$$\eta \frac{d\mathbf{R}_i}{dt} = \mathbf{F}_i^r + \mathbf{F}_i^p + \mathbf{F}_d, \quad (1)$$

where η is the damping constant. The vortex-vortex interaction force [17, 18] is $\mathbf{F}_i^r = \sum_{i \neq j}^{N_v} f_0 K_1(r_{ij}/\lambda) \hat{\mathbf{r}}_{ij}$, where $K_1(r)$ is the modified Bessel function, $r_{ij} = |\mathbf{r}_i - \mathbf{r}_j|$ is the distance between vortices i and j located at \mathbf{r}_i and \mathbf{r}_j , $\hat{\mathbf{r}}_{ij} = (\mathbf{r}_i - \mathbf{r}_j)/r_{ij}$, the unit of force is $f_0 = \Phi_0^2/2\pi\mu_0\lambda^3$, Φ_0 is the flux quantum, and the London penetration depth λ is the unit of length. This interaction is appropriate for stiff 3D vortices in relatively thick films where the film thickness d is much larger than λ but is

smaller than the Larkin-Ovchinnikov correlation length [19, 20]. Time is measured in units of $\tau = \eta/f_0$ and a molecular dynamics (MD) time step is equal to 0.02τ . We find identical results if smaller time steps are used. For a $0.1\mu\text{m}$ thick crystal of NbSe_2 , $f_0 = 6.78 \times 10^{-5}\text{N/m}$ and $\eta = 2.36 \times 10^{-11}\text{Ns/m}$ [21], so that $\tau = 0.35\mu\text{s}$. The pinning force \mathbf{F}_i^p arises from pinning sites which are modeled as attractive parabolic potentials of radius r_p and strength f_p : $\mathbf{F}_i^p = -\sum_{k=1}^{N_p} f_p(r_{ik}/r_p)\Theta(r_p - r_{ik})\mathbf{r}_{ik}$, where $r_{ik} = |\mathbf{r}_i - \mathbf{r}_k|$ is the distance between vortex i and pin k located at \mathbf{r}_k , $\hat{\mathbf{r}}_{ik} = (\mathbf{r}_i - \mathbf{r}_k)/r_{ik}$, and Θ is the Heaviside step function. The pinning interaction is intended to represent columnar pinning [22]. The net external driving force \mathbf{F}_d is comprised of the longitudinal force applied in the x -direction, $\mathbf{F}_d^L = F_d^L \hat{\mathbf{x}}$, and the transverse force applied in the y -direction, $\mathbf{F}_d^{Tr} = F_d^{Tr} \hat{\mathbf{y}}$. The vortex (pin) density is given by ρ_v (ρ_p). The system is prepared by simulated annealing, after which a longitudinal force is gradually applied in increments of $1 \times 10^{-4}f_0$ up to a specific value. The final longitudinal driving force is held fixed and then the transverse drive is applied in small increments. We measure the transverse velocity $V^{Tr} = \langle N_v^{-1} \sum_{i=1}^{N_v} \mathbf{v}_i \cdot \hat{\mathbf{y}} \rangle$, where \mathbf{v}_i is the velocity of vortex i . We also measure the fraction of sixfold coordinated vortices, $P_6 = N_v^{-1} \sum_{i=1}^{N_v} \delta(6 - z_i)$, where z_i is the coordination number of vortex i as determined from a Voronoi construction.

B. Sliding Wigner Crystals

The second system we consider is sliding Wigner crystals composed of N_e electrons. Here we use the same Langevin type simulations which were employed previously to identify the sliding states in this system [5]. The electron-electron interaction force $\mathbf{F}_i^r = -\nabla U_i^r$, where

$$U_i^r = \sum_{i \neq j}^{N_e} \frac{e^2}{|\mathbf{r}_i - \mathbf{r}_j|} \quad (2)$$

and $\mathbf{r}_{i(j)}$ is the location of electron $i(j)$. The electron crystal has lattice constant a_0 . The disorder comes from N_p positively charged impurities placed at a distance $d = 0.9a_0$ out of plane with the form $\mathbf{F}_i^p = -\nabla U_i^p$, where

$$U_i^p = -\sum_j^{N_p} \frac{e^2}{\sqrt{|\mathbf{r}_i - \mathbf{r}_j^{(p)}|^2 + d^2}}. \quad (3)$$

Here $\mathbf{r}_j^{(p)}$ is the in-plane projection of the location of pin j . The number of electrons N_e equals the number of impurities N_p . Both the electron-electron and electron impurity interactions are long range, and we evaluate them with a fast-converging sum [23]. To measure the transverse response, we follow a similar procedure as in the vortex system.

III. TRANSVERSE DEPINNING FOR VORTEX SYSTEMS

A. Definition of Pinning Regimes

We first consider a vortex system for a sample of size $L = 24\lambda$ with $\rho_v = \rho_p = 0.73/\lambda^2$, $r_p = 0.2\lambda$, and fixed longitudinal drive $F_d^L = 0.012f_0$. For this value of F_d^L and pinning density we find three regimes of the transverse response for varied pinning strength. For $f_p < 0.085f_0$ the system is in what we term the weak pinning limit, and the equilibrium state at $F_d^L = 0.0$ is free of dislocations. At $F_d^L = 0.012f_0$, there is a finite transverse depinning threshold and the transverse depinning occurs without the generation of additional defects. In the intermediate regime $0.085 \leq f_p/f_0 < 0.13$, the equilibrium $F_d^L = 0$ state contains dislocations, and for $F_d^L = 0.012f_0$ the transverse depinning is plastic and is accompanied by the generation of defects. Under a longitudinal drive, for $0.085 \leq f_p/f_0 < 0.106$ the vortices dynamically reorder into a defect-free lattice, while for $0.106 \leq f_p/f_0 < 0.13$ the vortices undergo a partial dynamical reordering into a moving smectic state containing a finite number of dislocations that are all aligned with the driving direction, as seen in previous simulations [6, 7]. The number of defects in the moving smectic state gradually increases with increasing f_p until each row of vortices is completely decoupled from the neighboring rows. A weak smectic state contains only a few dislocations so that several adjacent rows are coupled but rows separated by longer length scales are decoupled. In the strong pinning regime $f_p \geq 0.13f_0$, the vortices flow plastically through the system and the moving channel structure is destroyed so that the dislocations are no longer aligned with the drive. In this case there is no transverse depinning barrier. We have tested system sizes up to $L = 92\lambda$ and we find only dislocation free lattices in the equilibrium state for $f_p < 0.085f_0$. It is possible that for much larger systems than we can simulate, dislocations will eventually appear in the weak pinning systems.

B. Elastic Transverse Depinning

We consider a sample with $f_p = 0.06f_0$ in the weak pinning regime where the equilibrium lattice contains no dislocations. We fix the longitudinal drive to $F_d^L = 0.012f_0$ and increase F_d^{Tr} from zero in increments of $4 \times 10^{-5}f_0$ every 1.5×10^4 MD time steps. In order to resolve the steps in the transverse response, we average the transverse velocity V^{Tr} over 9×10^4 MD steps. The appearance of the curve does not change if V^{Tr} is averaged over 1.5×10^4 MD steps instead. A typical simulation runs for a total of more than 5×10^8 MD steps. When the net driving force vector aligns with a symmetry direction of the vortex lattice, we find that the transverse response locks to that direction over a range of F_d^{Tr} . For a moving triangular lattice, this locking occurs whenever

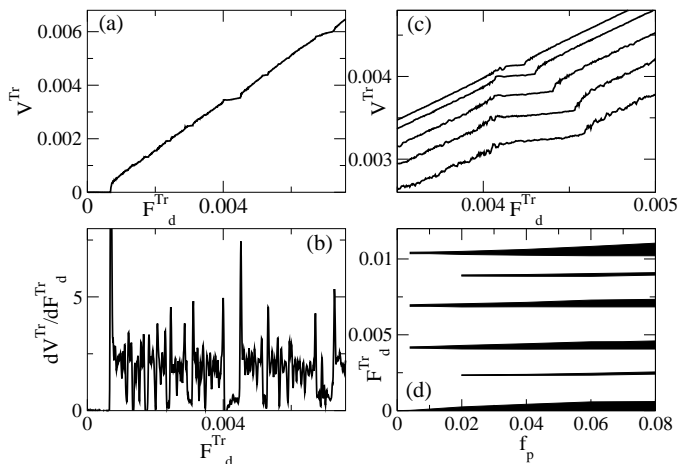


FIG. 1: (a) The transverse velocity V^{Tr} vs the transverse applied force F_d^{Tr} for a vortex lattice moving over random disorder of strength $f_p = 0.06f_0$ with fixed longitudinal driving force $F_d^L = 0.012f_0$. (b) dV^{Tr}/dF_d^{Tr} vs F_d^{Tr} for the same system. (c) V^{Tr} vs F_d^{Tr} showing the evolution of the (1, 2) step for $f_p = 0.02, 0.04, 0.06$, and $0.08f_0$, from top to bottom. (d) Step widths w_s in F_d^{Tr} vs f_p for the (0, 0), (1, 3), (1, 2), (3, 4), (3, 3) and (4, 4) steps, from bottom to top.

$F_d^{Tr}/F_d^L = \sqrt{3}m/(2n+1)$ where n and m are integers. In such a devil's staircase, the most pronounced steps occur when both n and m have low values.

The plot of V^{Tr} vs F_d^{Tr} in Fig. 1(a) shows that a transverse critical depinning threshold F_c^{Tr} occurs at $F_d^{Tr} = 0.00065f_0$. It is important to note that the vortex lattice remains aligned in the x -direction during the entire simulation. For increasing F_d^{Tr} , a number of steps appear in V^{Tr} corresponding to the locking of the net applied force vector with a symmetry direction of the lattice. A prominent step occurs near $F_d^{Tr} = 0.0043f_0$ which corresponds to the case of $(m, n) = (1, 2)$. The step at $F_d^{Tr} = 0.003f_0$ corresponds to the (1,3) state, and the (2,3) state appears at $F_d^{Tr} = 0.007f_0$. There are also a number of smaller steps at higher values of n and m , confirming the existence of a devil's staircase response. In Fig. 1(b), dV^{Tr}/dF_d^{Tr} vs F_d^{Tr} more succinctly highlights the steps. The peaks in Fig. 1(b) correspond to points at which the curvature in V^{Tr} vs F_d^{Tr} increases just before and after a plateau region. The most pronounced steps occur for (m, n) where the value of both m and n are small, which is typical for a devil's staircase structure. This result confirms the prediction of Giamarchi and Le Doussal [2] that if the moving lattice stays aligned with the original applied longitudinal drive, a devil's staircase response occurs due to the matching of the symmetry directions of the lattice with the applied drive.

The width of a given step w_s depends on the pinning strength and density. In Fig. 1(c) we illustrate the evolution of the (1, 2) step for $f_p/f_0 = 0.02, 0.04, 0.06$, and 0.08 , showing the growth of w_s with f_p . We also find that the step widths increase when the pinning density

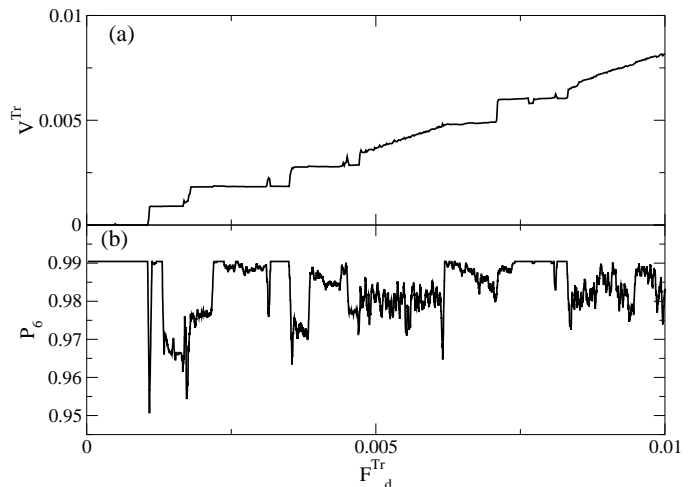


FIG. 2: (a) V^{Tr} vs F_d^{Tr} for a moving vortex lattice with the same parameters as in Fig. 1(a), but with $f_p = 0.106f_0$. (b) The fraction of six-fold coordinated vortices P_6 vs F_d^{Tr} for the same sample showing the correlations of the drops in P_6 with the transitions in V^{Tr} .

ρ_p is increased. In Fig. 1(d) we plot the evolution of w_s as a function of pinning strength for $(m, n) = (0, 0), (1, 3), (1, 2), (3, 4), (3, 3)$ and $(4, 4)$. We have verified that these results are robust up to systems of size $L = 60\lambda$ provided that the lattice remains free of dislocations. In two-dimensional pinned systems it has been argued that dislocations eventually appear at large distances even for weak disorder. These dislocations would limit the resolution of the devil's staircase, which should remain observable as long as the distance between dislocations is comparable to or greater than the system size.

C. Plastic Transverse Depinning

In the upper range of the intermediate pinning strength regime $0.106 \leq f_p/f_0 < 0.13$, the longitudinally driven vortices form a moving smectic state and the transverse depinning transition is *plastic*. Here the transverse velocity response is characterized by a series of sharp disordering-reordering transitions, giving rise to consecutive pronounced steps in V^{Tr} , as shown in Fig. 2(a) for a system with $f_p = 0.106f_0$. This ordering-disordering velocity-force response, which is distinct from a devil's staircase structure, occurs when the pinning is strong enough that the particles move in channels that are separated by a number of aligned dislocations, which is indicative of a smectic ordering. We also find two prominent peaks in the structure factor $S(\mathbf{k})$ consistent with a smectic state, as illustrated in Fig. 3. Here $S(\mathbf{k}) = N_v^{-1} |\sum_{i=1}^{N_v} \exp(-i\mathbf{k} \cdot \mathbf{r}_i)|^2$. In addition to the two prominent peaks, Fig. 3 shows the presence of four smaller peaks. Since $f_p = 0.106f_0$ falls at the edge of the regime where the moving smectic state forms, there are

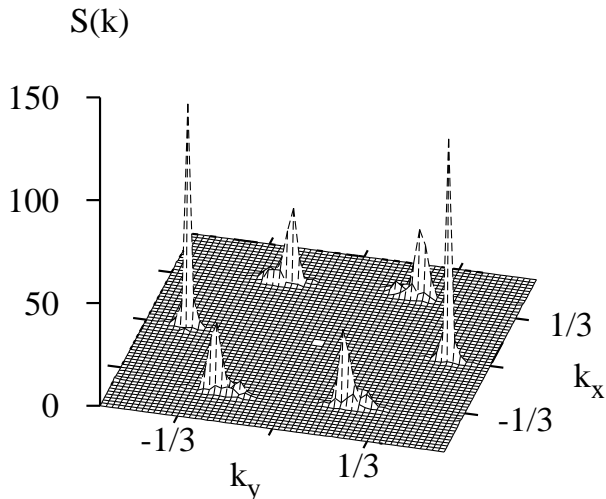


FIG. 3: Structure factor $S(\mathbf{k})$ for a system with $f_p = 0.106f_0$ in the moving smectic state at $F_d^{Tr} = 4 \times 10^{-4}f_0$ and $F_d^L = 0.012f_0$. The central peak is not shown.

only a small number of dislocations present in the moving smectic state and correlations between neighboring channels of vortices occur over a width of several channels. These correlations produce the four smaller peaks in $S(\mathbf{k})$. For larger system sizes L these four small peaks shrink in magnitude while the two prominent peaks remain prominent. In Ref. [6], the prominent peaks were observed to decay algebraically with system size and the state was termed a moving transverse Bragg glass. It is beyond the scope of this work to confirm the existence of a moving transverse Bragg glass. For larger values of f_p , the dislocation density in the moving smectic state increases, the correlation length between the moving vortex channels decreases to the width of a single channel, and only two peaks appear in $S(\mathbf{k})$. For $f_p > 0.13f_0$ the channel structure is destroyed and the vortices move plastically.

Since the transverse depinning process at $f_p = 0.106f_0$ is plastic, a large number of transient dislocations are induced at the depinning transition which destroy the well ordered channel structures. In Fig. 2(b) we plot the fraction of sixfold-coordinated vortices P_6 for the same system in Fig. 2(a), indicating that the changes in the behavior of V^{Tr} coincide with changes in P_6 . In the regions where V^{Tr} is increasing linearly with drive, P_6 drops and shows rapid fluctuations. Here, the 1D channel structure of the moving lattice is destroyed. We note that for $0.085 \leq f_p/f_0 < 0.106$ we do not observe any dislocations in the longitudinal moving lattice; however, since the system is close to the value of f_p at which dislocations appear in the longitudinally moving lattice, at the transverse depinning transition the extra strain on the lattice is enough to induce some dislocations and the system also depins plastically.

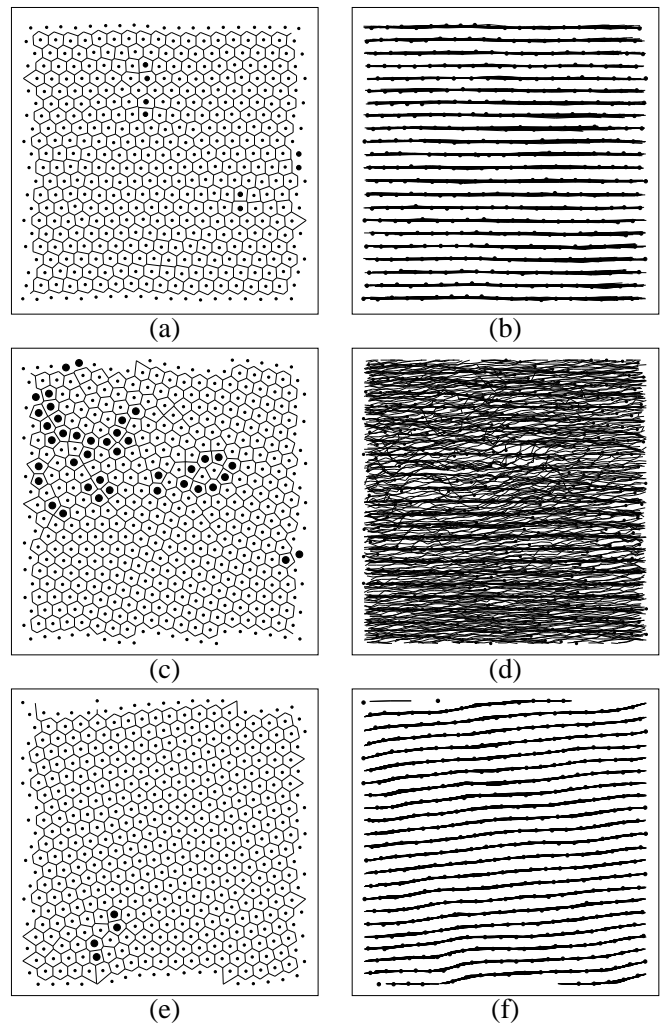


FIG. 4: (a,c,e): Voronoi construction for the vortex configurations for the system in Fig. 2 taken from a single snapshot. Small dots: sixfold-coordinated vortices; large dots: nonsixfold-coordinated vortices. (b,d,f): Vortex trajectories (black lines) during a fixed time span. (a,b): Transversely pinned state at $F_d^{Tr} = 4 \times 10^{-4}f_0$ where a clear channel structure appears. (c,d): The transition state at $F_d^{Tr} = 0.0011f_0$. (e,f): The state at the first plateau in V^{Tr} at $F_d^{Tr} = 0.00125f_0$ where the system has reorganized into a tilted channel structure.

To further illustrate the change in lattice structure that occurs on the steps in the intermediate pinning regime, in Fig. 4(a) we show the Voronoi construction of the vortex lattice from the system in Fig. 2 for a transversely pinned state at $F_d^{Tr} = 4 \times 10^{-4}f_0$. There are a small number of dislocations present, indicated by large dark circles, and all of the dislocation pairs are aligned with the direction of the drive (to the right in the figure). The vortex lattice is also aligned with the driving direction. In Fig. 4(b) the vortex positions (black dots) and trajectories (black lines) indicate that the motion is confined to well defined 1D channels. Above the transverse depinning transition,

illustrated in Fig. 4(c,d) for $F_d^{Tr} = 0.0011f_0$, numerous dislocations are present as indicated by Fig. 4(c), while the trajectories in Fig. 4(d) show that the channeling effect has been lost. This disordered type of flow appears both at the transitions among the higher steps as well as in the regions where V^{Tr} is increasing linearly.

In Fig. 2(a), the velocity jumps to a finite value and becomes locked onto a plateau for $0.0011f_0 < F_d^{Tr} < 0.0017f_0$. Here and on the other plateaus in V^{Tr} , the lattice moves in a channel structure which is aligned at an angle to the x direction, such as that shown in Fig. 4(e,f) for $F_d = 0.00125f_0$. As F_d^{Tr} increases, the system undergoes repeated plastic depinning transitions, each of which appears as a drop in P_6 . In the plastic flow region that follows each of these depinning transitions, the vortices move in the direction of the net force vector. As the transverse drive increases to a new plateau, the lattice reorders into a new channel structure which sets up a new transverse barrier to further increases in V^{Tr} .

The channels require some time to reform, so the width of the reordering transition as a function of transverse driving force is dependent on the sweep rate of F_d^{Tr} . For higher sweep rates, the width of the disordered regions between plateaus grows. In the adiabatic regime, the steps would be much sharper, suggesting that the transitions are first order in nature. We also find hysteresis in the steps when we reverse F_d^{Tr} . For very strong pinning, $f_p > 0.13f_0$, and fixed $F_d^L = 0.012f_0$, the channel structures are destroyed and the vortices flow plastically for all transverse drives; however, for higher values of F_d^L , a partially ordered phase appears and the transverse depinning occurs in the same manner as in Fig. 2. In general, for stronger disorder the longitudinal moving state contains numerous dislocations and the transverse depinning occurs in a step like fashion.

The transition between devil's staircase behavior at weak pinning and the order-disorder transitions associated with intermediate pinning strength is determined by the appearance of dislocations in the longitudinally driven lattice. In general, a devil's staircase appears when the disorder is weak enough that there are no dislocations present at any drive. For this reason, no evidence of a devil's staircase appeared in the simulations of Ref. [6], which showed the existence of a transverse depinning barrier. These simulations were performed in the intermediate pinning limit, as indicated by the linear scaling of f_c with the pinning strength in Ref. [6] and the presence of aligned dislocations in the lattice. The ordering-disordering steps that we find in the intermediate pinning limit were not observed in Ref. [6] since the resolution of the transverse force versus velocity curves was too low. The existence of a weak pinning regime may depend on system size. It has been argued that for any 2D system with random disorder, dislocations will always appear at sufficiently long length scales R_D even if the disorder is weak. In our simulations we have considered numerous different system sizes, and for $f_p < 0.085f_0$ we only observe dislocation free lattices. Due to computa-

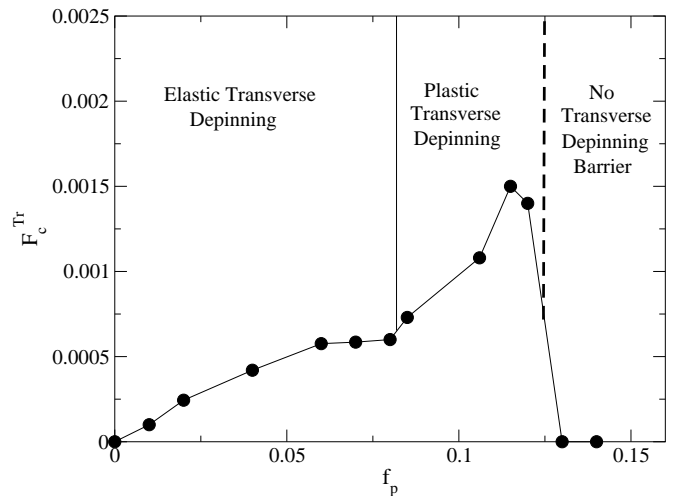


FIG. 5: F_c^{Tr} versus f_p for $F_d^L = 0.012f_0$ showing the three different response regimes. For weak pinning, $f_p < 0.085f_0$, the transverse depinning is elastic. For intermediate pinning, $0.085 \leq f_p/f_0 < 0.13$, the transverse depinning is plastic. There is no transverse depinning barrier for strong pinning $f_p \geq 0.13f_0$.

tional constraints we could only simulate systems of size $L = 92\lambda$ and less. It is possible that for much larger systems, dislocations will eventually appear. If enough dislocations are present to destroy the orientational order, the devil's staircase behavior would be lost when the well defined lattice directions of the moving lattice are lost. It is then possible that for system sizes $L < R_d$ the devil's staircase behavior will occur, while for $L > R_d$, the strong pinning behavior will be observed. On the other hand, if the system is in 3D with point pinning but with stiff vortices, than a 3D moving Bragg glass could form without dislocations, permitting a devil's staircase behavior to be observed for all lengths. We also note that the argument that dislocations will appear at some length scale R_d was made in the context of equilibrium systems. In the moving vortex case it may still be possible to obtain a defect free lattice in two dimensions as suggested by Koshelev and Vinokur [1].

In Fig. 5 we plot the transverse depinning barrier F_c^{Tr} vs f_p and indicate the three different pinning regimes which can be distinguished by the nature of the transverse response. In the weak pinning regime for $f_p/f_0 < 0.085$, the transverse depinning is elastic and a devil's staircase forms when F_d^{Tr} is swept. Within this regime, F_c^{Tr} increases monotonically with f_p . For the intermediate pinning regime $0.085 < f_p/f_0 < 0.13$, the transverse depinning is plastic and F_c^{Tr} is much higher than it was in the elastic depinning regime. For strong pinning $f_p/f_0 \geq 0.13$, the vortex lattice does not reorder when the longitudinal drive is applied, and the transverse depinning barrier disappears.

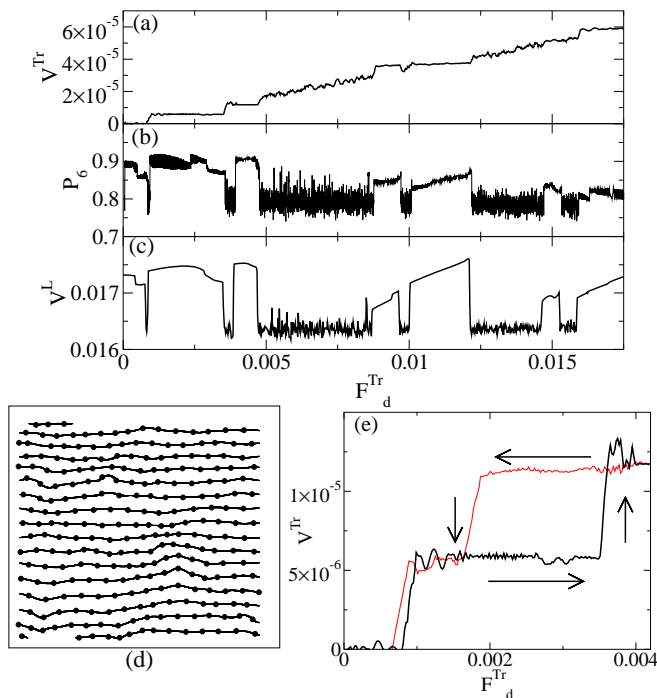


FIG. 6: (a) V^{Tr} vs F_d^{Tr} for a sliding Wigner crystal with fixed $F_d^L = 0.03$. (b) P_6 vs F_d^{Tr} . (c) V^L vs F_d^{Tr} . (d) The particle trajectories for the transversely pinned sliding state at $F_d^{Tr} = 3 \times 10^{-4}$. (e) The hysteresis in the V^{Tr} vs F_d^{Tr} curve. Lower curve: increasing F_d^{Tr} . Upper curve: decreasing F_d^{Tr} .

IV. TRANSVERSE DEPINNING FOR SLIDING WIGNER CRYSTALS ON SMOOTH POTENTIAL LANDSCAPES

We now consider the effect of a smoothly varying potential substrate of the type that arises in Wigner crystal systems for charge disorder. In general, with this type of disorder we observe much larger relative critical transverse depinning thresholds F_c^{Tr}/F_c^L than with short range pinning. For long range disorder F_c^{Tr}/F_c^L can be as high as 0.4, while for short range disorder it is less than 0.1 to 0.01. The effective shaking temperature T^{sh} , which arises from the rapidly fluctuating force caused by the pinning, for particles moving over short range random disorder at velocity V is $T^{sh} \propto 1/V$ [1]. At high drives, the effective temperature drops with increasing V , and the system can reorder. At lower drives, V is smaller and the system melts into the plastic flow phase. In the smectic phase, the transverse depinning barrier increases as the longitudinal drive is decreased [8] so that the maximum transverse barrier occurs just before the longitudinal drive is so low that the shaking temperature melts the lattice and F_d^{Tr} is lost. For long range, smoothly disordered substrates, there is no rapidly

fluctuating force so the concept of an effective temperature does not apply. This means that a partially ordered moving state can persist to drives much closer to the longitudinal depinning threshold than in the case of short range pinning.

In Fig. 6(d), the particle trajectories for the case of long range charge disorder show that the channels are much more meandering than in Fig. 4(b). In Fig. 6(a,b,c) we plot V^{Tr} , P_6 , and the longitudinal velocity V^L for the sliding Wigner crystal system with fixed $F^L = 0.03$. In this case the system initially forms a moving smectic system with $P_6 = 0.9$. A step structure appears in V^{Tr} . On the step, the particles are flowing in channels and P_6 shows only small fluctuations. In regions where V^{Tr} is linearly increasing, P_6 rapidly fluctuates around a lower value, indicating that the system is more disordered. The order-disorder transitions also affect V^L , which decreases and shows strong fluctuations in the disordered regimes. In the ordered regimes, there are few fluctuations in V^L and there is a trend for V^L to increase with F_d^{Tr} . This effect is similar to loading-unloading cycles of the type found in friction systems. In Fig 6(e) we illustrate the presence of hysteresis in V^{Tr} vs F_d^{Tr} , which gives evidence that the order-disorder transitions have a first order characteristic.

V. SUMMARY

In summary, using numerical simulations we have confirmed the prediction of Giamarchi and Le Doussal that a devil's staircase transverse response occurs for an elastic vortex lattice moving over random pinning when the net force vector aligns with the symmetry directions of the moving lattice. The devil's staircase response appears in the weak pinning regime when both the equilibrium state and the moving state are free of dislocations and the transverse depinning occurs elastically without the generation of defects. For intermediate pinning strengths, where the equilibrium state is dislocated and the vortices form a moving smectic state under a longitudinal drive, the transverse depinning occurs in a series of hysteretic order-disorder transitions where the system alternately becomes disordered and then reorganizes into channel structures that exhibit a transverse depinning threshold. In this case a series of pronounced steps in the transverse response appear. In the case where the quenched disorder is long-range and smoothly varying, the order-disorder transitions dominate the response to an increasing applied transverse force. These results are applicable to vortices and Wigner crystals moving over random disorder.

This work was supported by the U.S. Department of Energy under Contract No. W-7405-ENG-36.

[1] A.E. Koshelev and V.M. Vinokur, Phys. Rev. Lett. **73**, 3580 (1994).

[2] T. Giamarchi and P. Le Doussal, Phys. Rev. Lett. **76**,

- 3408 (1996); P. Le Doussal and T. Giamarchi, Phys. Rev. B **57**, 11356 (1998).
- [3] L. Balents, M.C. Marchetti, and L. Radzihovsky, Phys. Rev. Lett. **78**, 751 (1997); Phys. Rev. B **57**, 7705 (1998).
- [4] N. Markovic, M.A.H. Dohmen, and H.S.J. van der Zant, Phys. Rev. Lett. **84**, 534 (2000).
- [5] C. Reichhardt, C.J. Olson, N. Grønbech-Jensen, and F. Nori, Phys. Rev. Lett. **86**, 004354 (2001).
- [6] K. Moon, R.T. Scalettar, and G.T. Zimányi, Phys. Rev. Lett. **77**, 2778 (1996).
- [7] C.J. Olson and C. Reichhardt, Phys. Rev. B **61**, R3811 (2000).
- [8] H. Fangohr, P.A.J. de Groot, and S.J. Cox, Phys. Rev. B **63**, 064501 (2001).
- [9] M. Marchevsky, J. Aarts, P.H. Kes, and M.V. Indenbom, Phys. Rev. Lett. **78**, 531 (1997); A.M. Troyanosvki, J. Aarts, and P.H. Kes, Nature (London) **399**, 665 (1999).
- [10] E. Olive, J.C. Soret, P. Le Doussal, and T. Giamarchi, Phys. Rev. Lett. **91**, 037005 (2003).
- [11] C. Reichhardt and F. Nori, Phys. Rev. Lett. **82**, 414 (1999).
- [12] E. Granato and S.C. Ying, Phys. Rev. Lett. **85**, 5368 (2000); Phys. Rev. B **69**, 125403 (2004).
- [13] P.T. Korda, M.B. Taylor and D.G. Grier, Phys. Rev. Lett. **89**, 128301 (2002).
- [14] A. Gopinathan and D.G. Grier, Phys. Rev. Lett **92**, 130602 (2004).
- [15] C. Reichhardt and C.J. Olson Reichhardt, Phys. Rev. E **69**, 041405 (2004).
- [16] A.M. Lacasta, J.M. Sancho, A.H. Romero, and K. Lindenberg, Phys. Rev. Lett. **94**, 160601 (2005); J.P. Gleeson, J.M. Sancho, A.M. Lacasta, and K. Lindenberg, Phys. Rev. E **73**, 041102 (2006).
- [17] P.-G. de Gennes, *Superconductivity of Metals and Alloys* (Benjamin, New York, 1966).
- [18] M. Tinkham, *Introduction to Superconductivity* (MacGraw-Hill, New York, 1975).
- [19] A.I. Larkin and Yu.N. Ovchinnikov, J. Low Temp. Phys. **34**, 409 (1979).
- [20] A. Brass and H.J. Jensen, Phys. Rev. B **39**, 9587 (1989).
- [21] C.J. Olson Reichhardt, A. Libál, and C. Reichhardt, Phys. Rev. B **73**, 184519 (2006).
- [22] C. Reichhardt, C.J. Olson, J. Groth, S. Field, and F. Nori, Phys. Rev. B **53**, R8898 (1996); C.J. Olson, C. Reichhardt, and F. Nori, Phys. Rev. Lett. **81**, 3757 (1998).
- [23] N. Grønbech-Jensen, Int. J. Mod. Phys. C **8**, 1287 (1997).